Generating and analyzing non-diffracting vector vortex beams

Yanming Li[a], Angela Dudley[b], Thandeka Mhlanga[b], Michael J. Escuti[a] and Andrew Forbes[b]

[a]Department of Electrical and Computer Engineering, North Carolina State University, Raleigh, USA;
[b]CSIR National Laser Centre, PO Box 395, Pretoria 0001, South Africa

ABSTRACT

We experimentally generate non-diffracting vector vortex beams by using a Spatial Light Modulator (SLM) and an azimuthal birefringent plate (q-plate). The SLM generates scalar Bessel beams and the q-plate converts them to vector vortex beams. Both single order Bessel beam and superposition cases are studied. The polarization and the azimuthal modes of the generated beams are analyzed. The results of modal decompositions on polarization components are in good agreement with theory. We demonstrate that the generated beams have cylindrical polarization and carry polarization dependent Orbital Angular Momentum (OAM).

Keywords: vector beam, orbital angular momentum, optical vortex, Bessel beam

1. INTRODUCTION

We report the first experimental generation and analysis of non-diffracting vector vortex beams by using a SLM and an azimuthal birefringent plate (q-plate). The SLM generates scalar Bessel beams and the q-plate converts them to vector vortex beams. Both single order Bessel beam and superposition cases are studied. The polarization and the azimuthal modes of the generated beams are analyzed. We examine the azimuthally varying polarization by recording the beam profiles through an analyzer. We measure the OAM of each polarization components by doing a modal decomposition on the beams separated by a linear and a circular polarization beam splitter. The results are in good agreement with theory, showing different OAM in orthogonal circular polarizations and the corresponding OAM superposition in linear polarizations. The full analysis concludes that our generated beams have cylindrical polarization and carry polarization dependent OAM.

2. BACKGROUND

2.1 Vector beam

Polarization describes the vectorial nature of optical waves. Yet most correlated light beams in research have homogenous polarization thus scalar waves. The study on vector beams in which polarization is spatially inhomogenous has attracted much interest in recent years. One group of vector beams are linearly polarized with spatially varying and cylindrical symmetric polarization axis at cross-section, so called cylindrical vector beams.[1,2] On a Poincare sphere, the polarization of these beams occupies the equator. A more general class of vector beams with spatially varying polarization that spans the entire Poincare sphere has also been proposed and implemented recently.[3] The special properties of vector beams such as tight focusing has led to various application in optical imaging[4] and manipulation.[5] Various methods of generating vector beams have been proposed including spatially varying birefringent elements,[6,7] optical fibers,[8] and interferometric methods.[9]

2.2 Optical vortex

An optical vortex field has a helical phase front about a singularity, which carry OAM. These helical wavefronts have an azimuthal angular dependence of $\exp(\mathrm{i}l\phi)$ where l is the topological charge and ϕ is the azimuthal angle. Examples that carry OAM include Laguerre-Gaussian beams[10] and high-order Bessel beams.[11] The non-diffracting property of the Bessel beams makes them especially interesting in many applications.[12,13]

Further author information: Andrew Forbes: E-mail: AForbes1@csir.co.za

Laser Beam Shaping XIV, edited by Andrew Forbes, Todd E. Lizotte, Proc. of SPIE Vol. 8843, 884305
 · doi: 10.1117/12.2027249

2.3 Vector vortex beams

When the polarization singularity in a vector beam is also a phase singularity the beam becomes a vector vortex beam. By choosing a Bessel beam as the OAM-carrier, we can create a non-diffracting vector vortex beam. Prior experimental studies into the generation of non-diffracting vector vortex beams involved the use of interferometric techniques[14] or subwavelength structures as a grating,[15] an axicon,[16] or an azimuthal phase plate in conjugation with an axicon.[17]

In this work, we present a new method to generate and analyze non-diffracting vector vortex beams using geometric phase optics as the key elements.

3. THEORY

Geometric phase elements are a category of optical elements that work upon the geometric property of optical fields. A large subgroup utilize optical polarization in its vector space usually expressed by the Poincare sphere. Basically, when the polarization of light undergoes a change as a path on the Poincare sphere, the light gains an extra phase additional to the dynamic phase associated with optical path length. We exploit two key features of this geometric phase in this work. First, this phase is linearly proportional to polarization change, which is easily controlled by waveplate-like elements. Second, this phase is opposite for the two orthogonal circular polarization. A good example of geometric phase elements that creates a linear geometric phase is a Polarization Grating (PG) and its variations.[18–20] The very unique property that the phase profile has opposite signs for right and left circularly polarized light, 2Φ or -2Φ, makes geometric phase elements intrinsically ideal for creating and analyzing vector vortex beams, based on the following observation.

The vector vortex beam can be decomposed into two scalar vortex beams in orthogonal homogenous circular polarizations, where the absolute polarization topological charge coincident with that of the helical phase singularity. Reversely, two orthogonal circular polarized helical beams with opposite helical phase should superimpose to a vector vortex beam. This relation can be explained by simple Jones calculus:

$$\mathrm{e}^{\mathrm{i}l\phi}\begin{bmatrix}1\\ \mathrm{i}\end{bmatrix}+\mathrm{e}^{-\mathrm{i}l\phi}\begin{bmatrix}1\\ -\mathrm{i}\end{bmatrix}\Longleftrightarrow\begin{bmatrix}\cos(l\phi)\\ \sin(l\phi)\end{bmatrix} \tag{1}$$

The amplitude constants are omitted for the sake of simplicity.

The geometric phase element we used for generating vector vortex has a linear optical axis function in the azimuthal dimension $\Phi(\phi)=q\phi+\Phi_0$, which in many works is called a "q-plate".[21] For linear polarized input (with helical phase of charge l_0), the opposite phase is added to the right and left circular polarization components (Eq. 2a) and results in a vector vortex beam (Eq. 2b):

$$\mathrm{e}^{\mathrm{i}l_0\phi}\begin{bmatrix}1\\ 0\end{bmatrix}\xrightarrow{q\text{-plate}}\quad \mathrm{e}^{\mathrm{i}(l_0+2q)\phi}\begin{bmatrix}1\\ \mathrm{i}\end{bmatrix}+\mathrm{e}^{\mathrm{i}(l_0-2q)\phi}\begin{bmatrix}1\\ -\mathrm{i}\end{bmatrix} \tag{2a}$$

$$\Longleftrightarrow \mathrm{e}^{\mathrm{i}l_0\phi}\begin{bmatrix}\cos(2q\phi)\\ \sin(2q\phi)\end{bmatrix} \tag{2b}$$

$$\Longleftrightarrow (\mathrm{e}^{\mathrm{i}(l_0+2q)\phi}+\mathrm{e}^{\mathrm{i}(l_0-2q)\phi})\begin{bmatrix}1\\ 0\end{bmatrix}+\mathrm{i}(\mathrm{e}^{\mathrm{i}(l_0+2q)\phi}-\mathrm{e}^{\mathrm{i}(l_0-2q)\phi})\begin{bmatrix}0\\ 1\end{bmatrix} \tag{2c}$$

From the vector vortex beam expression (Eq. 2b) we can see that the topological charge of the azimuthally varying polarization is determined by the q-plate. For $q=1/2$, the resultant vector beams have a polarization singularity of charge 1, which includes the special cases of radial polarization and azimuthal polarization. Although this work is demonstrated with $q=1/2$, it can easily be extended to other q values.

Eq. 2c is the resultant beam decomposed into the linear polarization basis. It is shown that for each linear polarized component, two conjugate helical phase modes are present. Compare to the decomposition on the circular basis, we reveal an interesting characteristic of vector vortex beams, that is their helical mode decomposition result is dependent on the polarization choice. This is very different from scaler vortex beams, whose helical mode is independent on polarization.

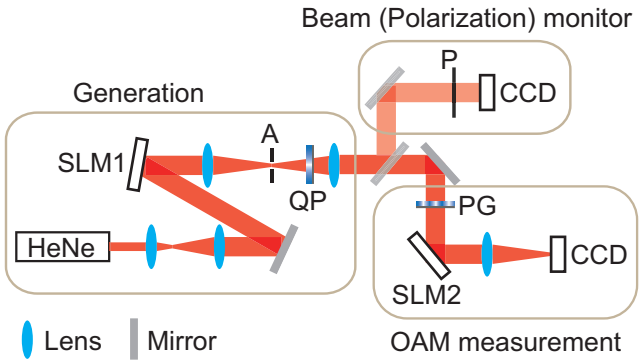

Figure 1. Experimental setup, including the vector vortex generation module, the beam profile and polarization monitor module, and the OAM measurement module. SLM–spatial light modulator; A–aperture; QP–q-plate; P–polarizer; PG–polarization grating; CCD–camera.

4. EXPERIMENTS

4.1 Experimental setup

The experimental setup is illustrated in Fig. 1. The spatial mode is prepared using a SLM. To generate scalar Bessel beams an expanded HeNe laser beam (633 nm) was directed onto the first SLM (SLM1). These fields were generated in a similar approach to Durnin's ring-slit aperture method,[22] implemented digitally[11] on SLM1 (HoloEye, PLUTO-VIS, with 1920×1080 pixels of pitch 8 μm and calibrated for a 2π phase shift at 633 nm) with the use of complex amplitude modulation.[23–25] An aperture at the Fourier plane selects the target Bessel beam. The q-plate is aligned to the beam to generate vector vortex Bessel beams.

The generated beam is analyzed separately by two modules with the help of a flippable mirror. The first module consist of an removable polarizer and a CCD camera. The beam intensity and polarization profile is acquired by the camera. In the setting shown in Fig. 1 the camera records the beam at the far-field. We also moved the module to the location at the aperture to record the beam at the near-field. The second module does an OAM decomposition using SLM2. We consider the modal decomposition of our input field E into azimuthal modes $\exp(\mathrm{i}l\phi)$ so that $E = \sum_l c_l \exp(\mathrm{i}l\phi)$. The modal weighting coefficients c_l may be found by the inner product of the field with an azimuthal match-filter, $c_l = |\langle E| \exp(\mathrm{i}l\phi)\rangle|$. The inner-product was executed experimentally by directing the modes onto the match-filter, encoded on SLM2 and viewing the Fourier transform, with the use of a lens, on the CCD (Spiricon BeamGage, SP620U). Since the SLM is only responsive to horizontal polarization, direct decomposition of the vector vortex beam is actually acting on the horizontal component (first term in Eq. 2c). To measure the two orthogonal circularly polarized scalar beams, we insert a PG before the decomposition. The PG acts as a circular polarizing beam splitter. The orientation of the PG is selected so that only right or left circularly polarized component is aligned to the SLM thus undergoing the azimuthal mode decomposition.

4.2 Cylindrical polarization

The first analysis on the generated beam is on its polarization. We first directly capture the beam intensity profile by the CCD camera before and after the q-plate, which correspond to the scalar Bessel beam from the SLM and the vector vortex Bessel beam generated by the q-plate, respectively. Then we insert a polarizer with an adjustable transmission axis to analyze the local polarization of the vector vortex Bessel beams. We captured all beams at their near-field and far-field (Fig. 2, first and third rows). Comparing the beams before and after the q-plate, we can see the beam center changes from a intensity peak to a minimum in the case of $l = 0$, which indicates that a singularity is created. In the case of $l = \pm 2$ the beam profile also changes, but since the singularity is complicated before and after, we will have a better understanding in the OAM decomposition section.

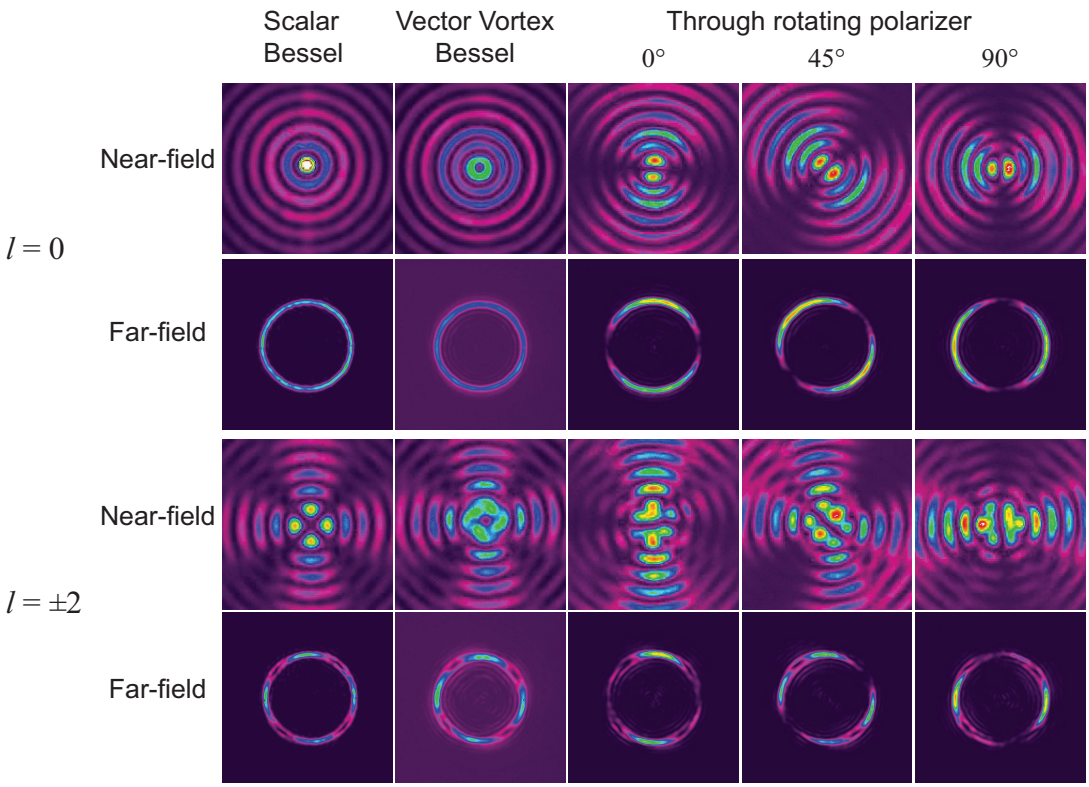

Figure 2. Beam profiles of two cases: input $l = 0$ (first and second row) and $l = \pm 2$ (third and fourth row). First column is the scalar Bessel from the SLM. Second column is the vector vortex Bessel from the q-plate. Third to fifth columns are the vector vortex Bessel beam captured with a rotating polarizer at 0 deg, 45 deg, and 90 deg, respectively. Both near-field (first and third row) and far-field (second and fourth row) are captured for each case.

The polarization of the vector vortex beams is verified azimuthally in Fig. 2. With a rotating polarizer, the transmitted portion of the beam rotates accordingly. This indicates an azimuthal polarization on the vector vortex beams. Comparing the cases of $l = 0$ and $l = \pm 2$, the local polarization orientation are the same. This result matchs the theoretical prediction (Eq. 2b) that the polarization topological charge is solely dependent on the q-plate used to generate the vector vortex beam and the value is double the q-plate charge. For the q-plate we use, $q = 1/2$, so the polarization has a singularity of charge 1, which is usually referred to as cylindrical polarization. This can easily be expanded to higher charges or some complex polarization distributions with the usa of different charge q-plates.

4.3 OAM decomposition results

The phase singularity is analyzed using azimuthal modal decomposition. Both the decomposition on linearly and circularly polarized components are presented in Fig. 3. In each subfigure the x-axis is the OAM charge of the input scalar beam from SLM1 and y-axis is the theoretical or experimentally measured OAM charge. The grey-scaled color in a block at (x, y) denotes the model weighting coefficient c_y with $l = x$ input scalar beam, where black is 0 and white is 1. First we have the decomposition results without PG shown in the first column. According to Eq. 2c, a single input of the OAM mode is transformed into two symmetric (about the input) OAM modes. The mode offset is decided by the q-plate charge. For our case, $q = 1/2$, the mode offset is ± 1. In the plot $c_y = 0.5$ only at locations where $y = x \pm 1$ and $c_y = 0$ elsewhere. We can see that the experimental results match the theoretical prediction. For each input mode, the weighting coefficient peaks at two adjacent modes. The two symmetric modes are measured to have nearly equal weighting, the slight difference is believed to come from the imperfect linear polarization at the input. A polarizer can be added to the path before the q-plate to

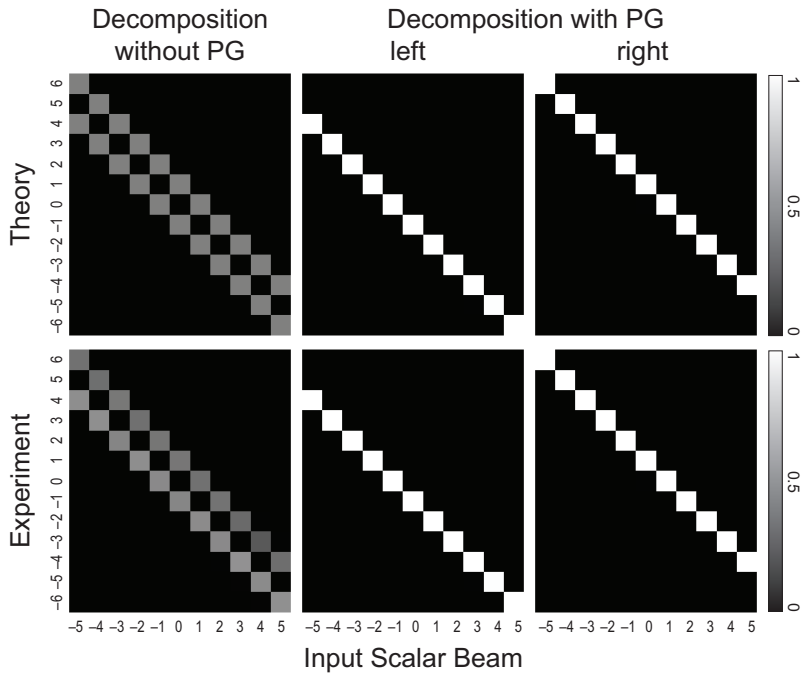

Figure 3. Theoretical (top row) and experimental (bottom row) azimuthal modal decomposition results. The OAM charge of the input (horizontal x-axis) and output (vertical y-axis) of q-plate is listed as a check board. The greyscale of each square denotes the modal weighting coefficient. The results taken without PG are shown in the first column, while results of the two sides of the PG are shown in the second (left) and third column (right).

improve the balance. We also want to point out that if one adds a quarter wave plate before the q-plate and adjusts its optical axis so that the input polarization to the q-plate is changed between linear and circular, the weight ratio between the two output modes can be adjusted accordingly. More details on this feature of q-plates can be found in the cited literatures.[21,26]

We then insert a PG before the camera and separate the orthogonal circular polarizations. The alignment is adjusted so that only the left or right circularly polarized component is captured each time. The results are summarized in the second and the third column in Fig. 3. The theoretical plots are generated according to Eq. 2a, only the $-1(+1)$ mode should appear for left(right) circularly polarized component and its weighting should be 1. The experimental results show two perfect diagonal lines which match the theory. Cross-talk is almost not measurable ($< 1\%$).

5. DISCUSSION

We have experimentally generated and analyzed non-diffracting vector Bessel beams. Digital holograms are used to control dynamic phase and create scalar vortex fields. An azimuthal wave plate is used to control geometric phase and convert these fields into cylindrical vector vortex fields. Although this work is focused on Bessel family spatial profiles and unit topological charge, the digital holograms are almost freely adaptable and the q-plate can be easily made with different configurations. Thus this method is very versatile and capable for the realization of a broad range of vector fields.

We detected the polarization of the generated vector field as well as their vortex nature by performing an azimuthal modal decomposition. In addition to their known classical applications, having the ability to simultaneously control the polarization and OAM degrees of freedom is useful in hyper-entanglement systems.

ACKNOWLEDGMENTS

The authors gratefully acknowledge the support from the US National Science Foundation (NSF and ECCS-0955127) and the National Research Foundation.

REFERENCES

[1] Youngworth, K. and Brown, T., "Focusing of high numerical aperture cylindrical-vector beams.," *Optics Express* **7**(2), 77–87 (2000).

[2] Zhan, Q., "Cylindrical vector beams: from mathematical concepts to applications," *Advances in Optics and Photonics* **1**(1), 1 (2009).

[3] Beckley, A. M., Brown, T. G., and Alonso, M. a., "Full Poincaré beams.," *Optics Express* **18**(10), 10777–85 (2010).

[4] Bokor, N. and Davidson, N., "Toward a spherical spot distribution with 4pi focusing of radially polarized light.," *Optics Letters* **29**(17), 1968–70 (2004).

[5] Zhan, Q., "Trapping metallic Rayleigh particles with radial polarization.," *Optics Express* **12**(15), 3377–82 (2004).

[6] Stalder, M. and Schadt, M., "Linearly polarized light with axial symmetry generated by liquid-crystal polarization converters.," *Optics Letters* **21**(23), 1948–50 (1996).

[7] Bomzon, Z., Biener, G., Kleiner, V., and Hasman, E., "Radially and azimuthally polarized beams generated by space-variant dielectric subwavelength gratings," *Optics Letters* **27**(5), 285–287 (2002).

[8] Grosjean, T., Courjon, D., and Spajer, M., "An all-fiber device for generating radially and other polarized light beams," *Optics Communications* **203**(1-2), 1–5 (2002).

[9] Maurer, C., Jesacher, A., Fürhapter, S., Bernet, S., and Ritsch-Marte, M., "Tailoring of arbitrary optical vector beams," *New Journal of Physics* **9**(3), 78–78 (2007).

[10] Allen, L., Beijersbergen, M., Spreeuw, R., and Woerdman, J., "Orbital angular momentum of light and the transformation of Laguerre-Gaussian laser modes," *Physical Review A* **45**(11), 8185–8189 (1992).

[11] Vasilyeu, R., Dudley, A., Khilo, N., and Forbes, A., "Generating superpositions of higher-order Bessel beams.," *Optics Express* **17**(26), 23389–95 (2009).

[12] Fahrbach, F., Simon, P., and Rohrbach, A., "Microscopy with self-reconstructing beams," *Nature Photonics* **4**(11), 780–785 (2010).

[13] Gatto, A., Tacca, M., Martelli, P., Boffi, P., and Martinelli, M., "Free-space orbital angular momentum division multiplexing with Bessel beams," *Journal of Optics* **13**(6), 064018 (2011).

[14] Milione, G., Evans, S., Nolan, D. a., and Alfano, R. R., "Higher Order Pancharatnam-Berry Phase and the Angular Momentum of Light," *Physical Review Letters* **108**(19), 190401 (2012).

[15] Bomzon, Z., Niv, A., Biener, G., Kleiner, V., and Hasman, E., "Nondiffracting periodically space-variant polarization beams with subwavelength gratings," *Applied Physics Letters* **80**(20), 3685 (2002).

[16] Tervo, J. and Turunen, J., "Generation of vectorial propagation-invariant fields by polarization-grating axicons," *Optics Communications* **192**(1-2), 13–18 (2001).

[17] Niv, A., Biener, G., Kleiner, V., and Hasman, E., "Propagation-invariant vectorial Bessel beams obtained by use of quantized Pancharatnam-Berry phase optical elements," *Optics Letters* **29**(3), 238–240 (2004).

[18] Escuti, M. J. and Jones, W. M., "Polarization-Independent Switching With High Contrast From A Liquid Crystal Polarization Grating," *SID Symposium Digest* **37**, 1443–1446 (2006).

[19] Li, Y., Kim, J., and Escuti, M. J., "Orbital angular momentum generation and mode transformation with high efficiency using forked polarization gratings.," *Applied Optics* **51**(34), 8236–45 (2012).

[20] Hasman, E., Bomzon, Z., Niv, A., Biener, G., and Kleiner, V., "Polarization beam-splitters and optical switches based on space-variant computer-generated subwavelength quasi-periodic structures," *Optics Communications* **209**(1-3), 45–54 (2002).

[21] Marrucci, L., Manzo, C., and Paparo, D., "Pancharatnam-Berry phase optical elements for wave front shaping in the visible domain: Switchable helical mode generation," *Applied Physics Letters* **88**(22), 221102 (2006).

[22] Durnin, J., Miceli Jr, J., and Eberly, J., "Diffraction-free beams," *Physical Review Letters* **58**(15), 1499–1501 (1987).

[23] Wong, D. and Chen, G., "Redistribution of the zero order by the use of a phase checkerboard pattern in computer generated holograms," *Applied Optics* **47**(4), 602–610 (2008).

[24] López-Mariscal, C. and Helmerson, K., "Shaped nondiffracting beams," *Optics Letters* **35**(8), 1215–1217 (2010).

[25] Dudley, A., Vasilyeu, R., Belyi, V., and Khilo, N., "Controlling the evolution of nondiffracting speckle by complex amplitude modulation on a phase-only spatial light modulator," *Optics Communications* **285**(1), 5–12 (2012).

[26] Li, Y., Kim, J., and Escuti, M. J., "Controlling orbital angular momentum using forked polarization gratings," *Proc. SPIE* **7789**, 77890F (2010).